Russian Journal of General Chemistry, Vol. 73, No. 5, 2003, pp. 765–775. Translated from Zhurnal Obshchei Khimii, Vol. 73, No. 5, 2003, pp. 809–820.

Quantum-Chemical Study of Adducts of Silicon Halides with Nitrogen-containing Donors: IV.[1] Adducts with Pyridine

A. Yu. Timoshkin, T. N. Sevast'yanova, E. I. Davydova, A. V. Suvorov, and H. F. Schaefer

St. Petersburg State University, St. Petersburg, Russia

Center for Computational Quantum Chemistry, University Of Georgia, USA

Received December 17, 2001

Abstract — The structural and thermodynamic characteristics of $SiX_4 \cdot Py$ and $SiX_4 \cdot 2Py$ adducts (X = H, F, Cl, Br) were calculated by *ab initio* and DFT methods (RHF and B3LYP). The resulting data were used to estimate for the first time the enthalpies of sublimation of *trans*-$SiX_4 \cdot 2Py$ complexes. The distortion energies of the donor and acceptor fragments and the energies of the Si–N bonds in the 1 : 1 and 1 : 2 halide complexes were calculated. The high distortion energy makes thermodynamically unfavorable equatorial monopyridine adducts with Si–N bond energies of 150–200 kJ/mol. In *trans* 1 : 2 complexes, pyridine acts as a weaker donor than ammonia with respect to silicon tetrahalides.

Our previous quantum-chemical calculations of the structural and thermodynamic characteristics of $SiX_4 \cdot NH_3$ and $SiX_4 \cdot 2NH_3$ adducts (X = H, F, Cl, Br) as model systems [1–3] allowed us to work out the calculation technique, to analyze the effects of X on the Si–N and Si–X bond lengths, effective atomic charges, dissociation enthalpies, and silicon–nitrogen bond energies in the ammonia adducts. Consideration of the structural and energetic parameters of the ammonia complexes point to distortion of the initial molecules and to necessity of inclusion of the distortion energy in the calculation of the energies of donor–acceptor bonds [3].

To compare the calculated and experimental data, we should consider systems with more stable, actually existing adducts. These systems require a more powerful donor, with which processes similar to ammonolysis [1] are less favored than adduct formation. Pyridine (Py) is one of such donors. Its 1 : 2 adducts with silicon halides have been sufficiently well studied experimentally but are hardly amenable to quantum-chemical calculations.

In this work we performed quantum-chemical calculations of 1 : 1 and 1 : 2 adducts of SiX_4 (X = H, F, Cl, Br) and pyridine to reveal the effect of the nature of the halogen and nitrogen-containing donor on the structural and energetic characteristics of the adducts. These calculations make it possible to follow changes in the characteristics of the Si–X and Si–N bonds with changing silicon coordination number and element X. Joint consideration of pyridine and ammonia complexes allows us to compare the energies of Si–N donor–acceptor bonds for a wide range of adducts and to discuss the contribution of the distortion energy into the enthalpy of gas-phase dissociation of similar silicon halide adducts.

Published quantum-chemical calculations for adducts of silicon halides with pyridine are few in number [4–7]. Rami and Hansen [4] have calculated the energies of silicon–nitrogen $(d–p)_\pi$ bonding in $SiX_4 \cdot 2Py$ complexes (X = F, Cl) by the Hückel MO method and failed to unambiguously decide between the *cis* and *trans* configurations of the complexes. Semiempirical calculations of silicon tetrachloride complexes with pyridine have also been reported [5, 6]. The RHF and B3LYP *ab initio* calculations for a six-coordinate complex of dichlorosilane with pyridine [7] showed that a *trans*-octahedral $SiH_2Cl_2 \cdot (Py)_2$ adduct is energetically unfavored in the gas phase. According to Hensen *et al.* [7], this complex exists in the crystal state due to intermolecular hydrogen bonding between the chlorine and pyridine hydrogen atoms.

Like in [1–3], we performed all calculations at the Center for Computational Quantum Chemistry, University of Georgia (USA), using a standard GAUSSIAN 94 program package [8]. RHF self-consistent field and B3LYP density functional theory with the exchange functional B3 by Becke [9] and the correlation functional by Lee, Yang, and Parr [10] were applied. A full-electron basis set with d95** polarization func-

[1] For communication III, see [1].

1070-3632/03/7305-0765 $25.00 © 2003 MAIK "Nauka/Interperiodica"

Table 1. Structural characteristics of $SiX_4 \cdot Py$ complexes, calculated by the RHF and B3LYP methods[a]

Parameter	X = F				X = Cl, C_2		X = Br, C_2	
	C_1		C_2					
	RHF	B3LYP	RHF	B3LYP	RHF	B3LYP	RHF	B3LYP
l_{Si-N}	2.146	2.125	1.950	1.981	1.925	1.956	1.921	1.954
l_{Si-X}	1.591	1.622	1.599	1.625	2.099	2.109	2.255	2.282
$l_{Si-X'}$	1.604	1.630	1.642	1.670	2.200	2.207	2.404	2.403
l_{H-X}	2.654	2.208	2.109	2.080	2.905	2.910	3.157	3.109
∠XSiX	116.2	116.3	124.6	123.6	127.0	126.9	125.6	126.7
	119.7	119.9						
∠XSiX'	97.2	97.0	91.9	92.2	91.6	92.0	91.8	92.1
	96.4	96.1	92.1	92.4	91.6	91.9	91.9	92.1
∠X'SiX'	–	–	171.4	170.3	172.8	171.3	171.9	170.6

[a] Hereinafter, distances in Å and angles in degrees. Position of pyridine: C_1 axial and C_2 equatorial.

tions [11] was used with H, N, F, Si, and Cl atoms and the pVDZ full-electron basis set [12], for Br atoms. The calculation technique has been described in detail in [2].

The geometry of all the compounds (except for two of them) was fully optimized, and vibrational analysis was then performed. We failed to optimize the geometry of equatorial $SiH_4 \cdot Py$ and *cis*-$SiH_4 \cdot 2Py$. Structural characteristics are given for both the calculation methods. The enthalpies of processes were corrected for zero-point vibrational energies and reduced to the standard conditions using thermal corrections. In the latter case, only B3LYP results were used, since, as shown in [2], this method provides more reliable thermodynamic characteristics that the RHF method.

Compounds $SiX_4 \cdot Py$. The trigonal-bipyramidal geometry of $SiX_4 \cdot Py$ adducts with axial (C_1 or C_s symmetry) and equatorial (C_2 symmetry) pyridine molecules was optimized (Figs. 1a and 1b). The calculated Si–N distances for X = H in the axial isomers of $SiX_4 \cdot Py$ compare with the sum of the van der Waals radii of silicon and nitrogen, and for X = Cl and Br they are even longer by 0.2–0.6 Å. The calculated Si–X distances coincide with l_{SiX} in the initial molecules, the XSiX bond angles are close to tetrahedral, and no transfer of electron density on the acceptor takes place in the case of X = Cl, Br, whereas at X = H it does not exceed 0.03 *e*. These facts show that it makes no sense to consider $SiX_4 \cdot Py$ (X = H, Cl, Br) species with axial arrangement of the donor as independent molecular formations.

By contrast, in isomers with equatorial arrangement of pyridine in the trigonal bipyramid, the Si–N distance is shorter than the sum of the van der Waals radii and decreases along the series F, Cl, and Br. Furthermore, halides are noticeably distorted: The Si–X distances increase, the XSiX bond angles between equatorial halogen atoms also increase, and the same angles between equatorial and axial atoms decrease. Together these findings point to a donor–acceptor bond in these complexes. The calculated data are given in Table 1 (according to Fig. 1, X and X' denote equatorial and axial positions, respectively).

The fluoride complex is a special case. All its structural characteristics (Si–N and Si–X distances and bond angles) imply that $SiF_4 \cdot Py$ can have pyridine both equatorial and axial (Table 1), but the Si–N distances in the equatorial isomer are shorter by 0.15 Å than in the axial isomer.

Thus, our calculations showed that in pyridine complexes, as differentiated from ammonia complexes [2], the equatorial position of the ligand in the trigonal-bipyramidal configuration is preferred over axial.

The calculated distances between the halogen atoms and their nearest pyridine hydrogen atoms (l_{H-X}, Table 1) are shorter than the sums of the van der Waals radii of hydrogen and halogen (by 0.47 for fluoride, by 0.1 for chloride, and by 0.04 Å for bromide), implying intramolecular hydrogen bonding that stabilizes the C_2 structure. This fully agrees with the above-mentioned possibility of hydrogen bonding in crystalline adducts [7].

Changes in atomic charges in adducts $SiX_4 \cdot Py$ with respect to the initial halides are shown in Fig. 2a. It is clearly seen that the total negative charge on SiX_4

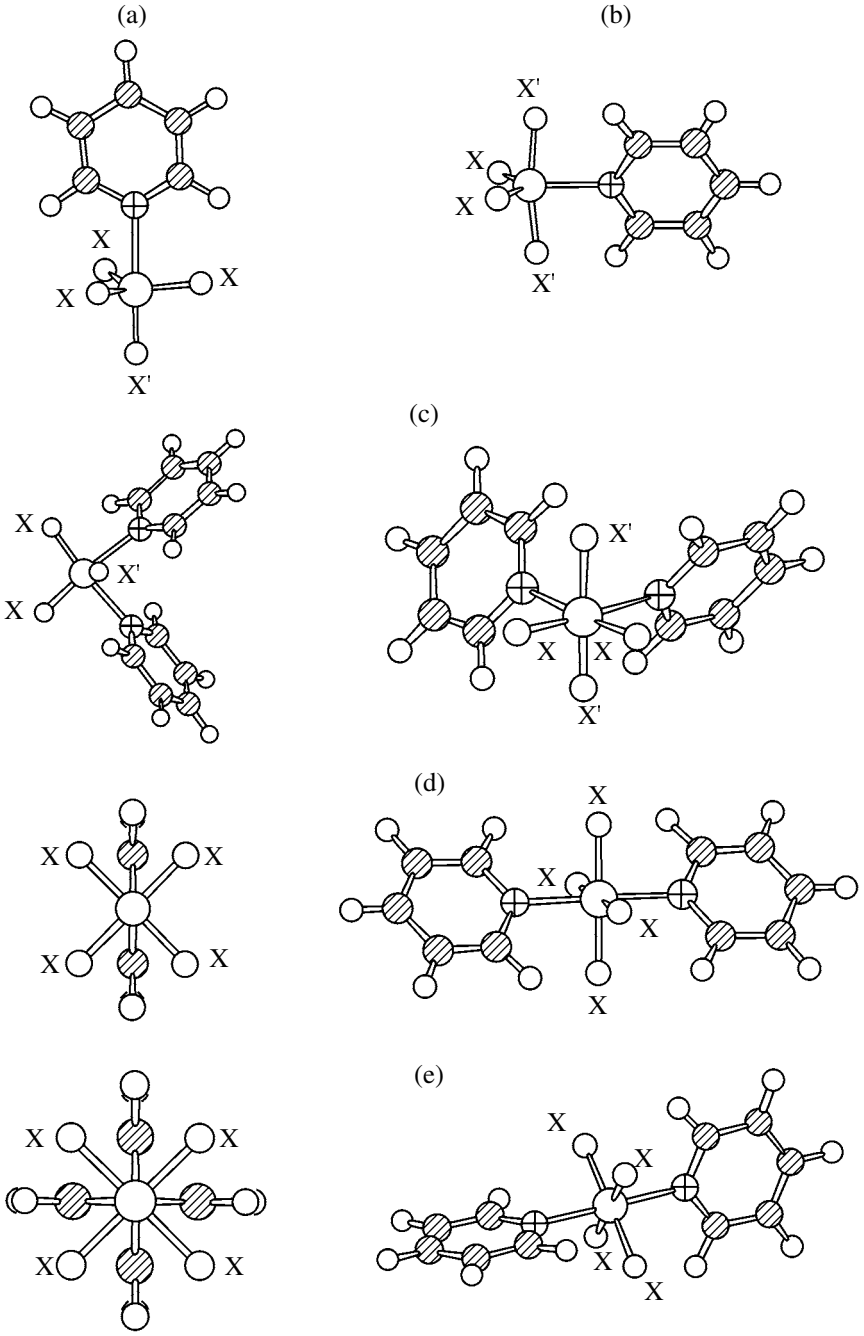

Fig. 1. Geometry of (a) axial $SiX_4 \cdot Py$, (b) equatorial $SiX_4 \cdot Py$, (c) *cis*-$SiX_4 \cdot 2Py$, (d) *trans*-$SiX_4 \cdot 2Py$ (D_{2h}), and (e) *trans*-$SiX_4 \cdot 2Py$ (D_{2d}).

increases in the series F, Cl, and Br. The characteristics of the silicon chloride and bromide adducts are close to each other and much differ from those of the fluoride adduct. The most essential differences are in the changes of the charge on the silicon and axial halogen atoms. The Δq_{Si} value for the chloride is positive, and for the fluoride it is negative. The changes in the charge on the fluorine atoms are much larger then on the chlorine and bromine atoms. Similar trends in Δq_{Si} and Δq_X we earlier observed in ammonia adducts $SiX_4 \cdot NH_3$ [2]. Feshin and Kon'shin [5] noted similar changes in the charge on the silicon atom in a trigonal-bipyramidal chloride complex with equatorial ligand arrangement. Apparently, distinctions in charge redistribution adducts of fluorides and other halides is rather common.

According to [5], the complex-forming centers Si

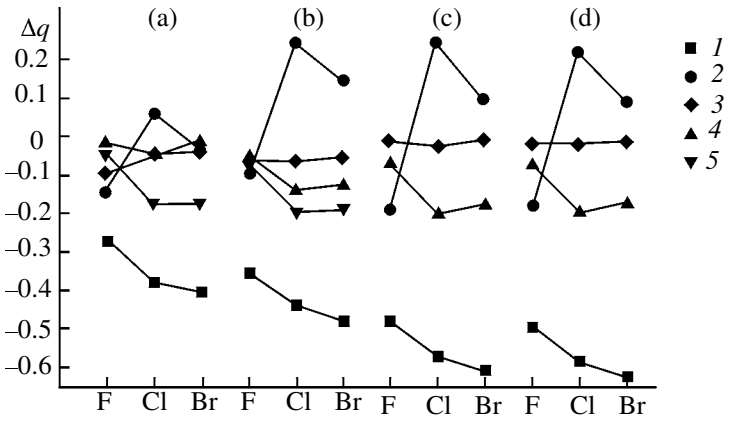

Fig. 2. Charge transfer to SiX_4 and change in effective atomic charges. (a) Equatorial $SiX_4 \cdot Py$, (b) *cis*-$SiX_4 \cdot 2Py$, (c) *trans*-$SiX_4 \cdot Py$ (D_{2d}), and (d) *trans*-$SiX_4 \cdot 2Py$ (D_{2h}). (*1*) SiX_4, (*2*) Si, (*3*) N, (*4*) X, (*5*) X′ {in all cases, $\Delta q(SiX_4) = q[SiX_4(SiX_4 \cdot nPy)] - q(SiX_4)$. For Si, X, and X′(E), $\Delta q_E = q_E(SiX_4 \cdot nPy) - q_E(SiX_4)$, and for N, $\Delta q_E = q_E(SiX_4 \cdot nPy) - q_E(Py)$}.

Table 2. Thermodynamic characteristics of gas-phase dissociation of $SiX_4 \cdot nPy$ adducts

X	ΔH^0_{298}(calc.), kJ/mol	ΔS^0_{298}(calc.), J mol^{-1} K^{-1}	X	ΔH^0_{298}(calc.), kJ/mol	ΔS^0_{298}(calc.), J mol^{-1} K^{-1}
	$SiX_4 \cdot Py_{eq} \longrightarrow SiX_4$			$SiX_4 \cdot 2Py(D_{2d}) \longrightarrow SiX_4 + 2Py$	
F	4.2	148.3	F	91.8	333.8
Cl	–53.4	146.5	Cl	11.7	348.8
Br	–58.5	145.4	Br	–7.8	347.4
	cis-$SiX_4 \cdot 2Py \longrightarrow SiX_4 \cdot Py_{eq} + Py$			$SiX_4 \cdot 2Py(D_{2h}) \longrightarrow SiX_4 + 2Py$	
F	65.0	182.6	F	89.1	329.2
Cl	34.5	191.6	Cl	11.7	348.9
Br	22.0	195.1	Br	–6.9	348.3
	$SiX_4 \cdot 2Py(D_{2d}) \longrightarrow SiX_4 \cdot Py_{eq} + Py$			$SiF_4 \cdot Py_{ax} \longrightarrow SiF_4 + Py$	
F	87.5	184.9		36.8	133.9
Cl	65.2	202.4			
Br	50.7	202.0			
	$SiX_4 \cdot 2Py(D_{2h}) \longrightarrow SiX_4 \cdot Py_{eq} + Py$			*cis*-$SiF_4 \cdot 2Py \longrightarrow SiF_4 \cdot Py_{ax} + Py$	
F	84.9	180.9		32.4	196.9
Cl	65.1	202.4			
Br	51.6	202.9			
	cis-$SiX_4 \cdot 2Py \longrightarrow SiX_4 + 2Py$			$SiF_4 \cdot 2Py(D_{2d}) \longrightarrow SiF_4 \cdot Py_{ax} + Py$	
F	69.2	330.8		55.0	199.3
Cl	–18.9	338.1		$SiF_4 \cdot 2Py(D_{2h}) \longrightarrow SiX_4 \cdot Py_{ax} + Py$	
Br	–36.4	340.5		52.3	195.3

and N do no more than initiate and transmit charge transfer. In fact, in the case of silicon chloride and bromide, the electron density from the nitrogen atom of the donor molecule is localized not on the silicon atom but is transferred on the halogen atoms. As a result of enhanced polarization of the molecule, not only the electron density transferred from the ligand, but also part of the electron density of the silicon atom is localized on the halogen atoms. By contrast, in the case of silicon tetrafluoride, the electron density is accepted by the silicon atom and only slightly transferred to the electron-saturated fluorine atoms.

Apart from structural parameters of the adducts, by the B3LYP method we found thermodynamic characteristics of their dissociation by Eq. (1).

$$SiX_4 \cdot Py(gas) = SiX_4(gas) + Py(gas). \quad (1)$$

Table 3. Structural characteristics of the *cis* forms of $SiX_4 \cdot 2Py$ complexes, calculated by the RHF and B3LYP methods

Parameter	X = F		X = Cl		X = Br	
	RHF	B3LYP	RHF	B3LYP	RHF	B3LYP
l_{Si-N}	2.098	2.103	2.135	2.145	2.128	2.149
l_{Si-X}	1.624	1.650	2.150	2.165	2.340	2.355
$l_{Si-X'}$	1.648	1.682	2.195	2.220	2.398	2.421
∠X'SiX'	163.4	163.2	170.5	169.8	172.9	171.6
∠XSiX	99.5	99.8	97.1	97.6	96.0	96.7
∠NSiN	87.0	86.8	84.4	84.4	84.2	83.9
∠X'SiN^1	84.0	84.0	86.3	86.1	87.0	86.6
∠X'SiN^2	84.0	83.9	86.7	86.4	87.7	87.2
∠XSiN^1	173.7	173.5	173.6	173.4	174.1	173.6
∠XSiN^2	86.9	86.7	89.2	89.0	89.9	89.7
∠XN^{1}N^{2}X	0.8	0.6	0.1	0	0.4	0.1

Table 4. Structural characteristics of the *trans* forms of $SiX_4 \cdot 2Py$ complexes, calculated by the RHF and B3LYP methods

Parameter	X = H				X = F				X = Cl				X = Br			
	D_{2h}		D_{2d}		D_{2h}		D_{2d}		D_{2h}		D_{2d}		D_{2h}		D_{2d}	
	RHF	B3LYP	RHF	B3LYP	RHF	B3LYP	RHF	B3LYP	RHF	B3LYP	RHF	B3LYP	RHF	B3LYP	RHF	B3LYP
l_{Si-N}	2.064	2.034	2.064	2.036	1.973	1.980	1.970	1.976	2.030	2.042	2.031	2.043	2.044	2.063	2.049	2.067
					1.93 [13][a]					1.976 [14][a]						
l_{Si-X}	1.552	1.564	1.551	1.564	1.660	1.689	1.660	1.690	2.201	2.219	2.202	2.219	2.397	2.414	2.396	2.413
					1.64 [13][a]					2.183 [14][a]						
∠SiX	89.4	89.1			89.2	89.2			90.7	90.4			91.2	90.9		

[a] Experimental data.

The ΔH^0_{298}(calc.) and ΔS^0_{298}(calc.) values for various processes given in Table 2 for structurally stable equatorial isomers of $SiX_4 \cdot Py$ adducts demonstrate that at X = Cl and Br these isomers are thermodynamically unstable, because their ΔH^0_{298}(calc.) values are strongly exothermic.

Thus, of $SiX_4 \cdot Py$ adducts, only $SiF_4 \cdot 2Py$ can exist, even though for the most thermodynamically stable axial isomer of the latter the temperature at which the equilibrium constant of process (1) is equal to unit ($T_{K=1}$) is as low as 275 K. This result explains the absence of experimental data for $SiX_4 \cdot Py$ adducts.

Compounds $SiX_4 \cdot 2Py$. For $SiX_4 \cdot Py$ complexes we optimized *cis* (C_2 symmetry; Fig. 1c) and *trans* isomers (D_{2d} and D_{2h} symmetry; Figs. 1d and 1e). The resulting data are listed in Tables 3 and 4. The Si–N distance in the six-coordinate $SiX_4 \cdot 2Py$ adducts are slightly longer than in the five-coordinate $SiX_4 \cdot Py$ adducts. Note that the Si–N distance in 1 : 2 ammonia adducts at all X is decreased compared with that in 1 : 1 adducts [1].

In all the *cis* complexes, the Si–N distance (Table 3) increases in the series F, Cl, and Br, but still is invariably shorter than the sum of the van der Waals radii of silicon and nitrogen (3.54 Å). The Si–Hal distances are longer than in the pure halides, and the Si–X distances are shorter than the Si–X' distances. Bond angles in the *cis* adducts change only slightly with halogen, and the plane formed by the nitrogen atoms and equatorial halogens atoms is distorted by 0.1–0.8°, depending on halogen and computational method.

The negative charge on the SiX_4 fragment increases in the series F, Cl, and Br (Fig. 2b); it is higher than

in the corresponding monopyridine adducts. The general trends in the charges on nitrogen, silicon, and halogen atoms are the same as in the monopyridine adducts.

In all the *trans* isomers, the Si–N distance (Table 4) is even shorter than in the corresponding *cis* isomers and increases in the series F, Cl, and Br. The Si–X distances are increased compared with the individual halides and *cis* isomers. The XSiX angles in the case of the D_{2d} symmetry are 90°, whereas in the case of the D_{2h} symmetry they differ from 90° by 0.4–1.2°, depending on halogen and computational method. The NSiN angle is 180° at all X both in the D_{2h} and D_{2d} complexes, and the N–Si–N straight line is perpendicular to the plane defined by the halogens atoms.

We have also calculated geometrical parameters for the *trans* isomer of the hydride adduct (Table 4). Though the Si–N distance in it compares with the Si–N distance in the chloride and bromide adducts, noteworthy is the fact that for the hydride adduct the B3LYP method gives shorter distances than the RHF method. This circumstance, as noted earlier [2], points to the importance of electron correlation effects for quantum-chemical description of these molecules. Therefore, having in mind that the *trans* isomers of $SiH_4 \cdot 2Py$ can in principle exist, in what follows we will deal with halide adducts only.

In the *trans* isomers, the character of charge transfer in the SiX_4 fragment and Si, X, and N atoms (Figs. 2c and 2d) is similar to that in the monopyridine adducts and *cis* isomers. This finding suggests that the above-described mechanism of electron density redistribution is preserved with adducts of any composition and structure.

Comparison of the total energies ΔE^0_{tot} shows that the *trans* isomers are preferred over the *cis* isomers by 23 (X = F), 31 (X = Cl), and 29–30 kJ/mol (X = Br). The D_{2d} configuration is preferred over D_{2h} by 2.9 kJ/mol for X = F and by as little as 0.1 kJ/mol, and for X = Br, vice versa, the D_{2h} configuration is preferred over D_{2d} by 0.9 kJ/mol.

Thermodynamic characteristics of the dissociation of the 1 : 2 adducts by Eqs. (2) and (3) are given in Table 2.

$$SiX_4 \cdot 2Py_{(cis,trans)}(\text{gas}) = SiX_4 \cdot Py_{\text{eq}}(\text{gas}) + Py(\text{gas}), \quad (2)$$

$$SiX_4 \cdot 2Py_{(cis,trans)}(\text{gas}) = SiX_4(\text{gas}) + 2Py(\text{gas}). \quad (3)$$

In the case of the fluoride, Eq. (4) is also possible.

$$SiF_4 \cdot 2Py_{(cis,trans)}(\text{gas}) = SiF_4 \cdot Py_{\text{ax}}(\text{gas}) + Py(\text{gas}). \quad (4)$$

As seen from the data in Table 2, adducts $SiX_4 \cdot 2Py$ all are stable [ΔH^0_{298}(calc.) > 0] with respect to processes (2). All forms of fluoride adducts are stable, and those of bromide adducts unstable with respect to processes (3).

Thus, comparison of the dissociation enthalpies of the adducts shows that the bromide adducts are thermodynamically unstable, and the *trans* isomers of the fluoride and chloride adducts are more stable than the *cis* isomers. This conclusion agrees with the results in [5]. Experimental evidence for the actually existing crystalline fluoride [13] and chloride [14] adducts, too, point to their *trans* configuration.

Thermal studies of adducts of silicon tetrahalides with pyridine [15–19] showed that heating in a vacuum or an inert solvent produces heterolytic cleavage of the Si–N bond. The thermochemistry of the pyridine adducts was studied by tensimetry [17, 19], calorimetry [20–23], and quantitative thermography [24]. Analysis of published data allowed us to estimate the most reliable enthalpy characteristics of process (5).

$$SiX_4 \cdot 2Py(\text{s.}) \longrightarrow SiX_4(\text{gas}) + 2Py(\text{gas}). \quad (5)$$

For the fluoride, chloride, and bromide adducts, $\Delta H^0(5)$ were estimated at 273 ± 2, 231 ± 4, and 237 ± 2 kJ/mol, respectively.

Comparison of the calculated characteristics of the complete gas-phase dissociation of the *trans* isomers by Eq. (3) with the experimental parameters relating to the dissociation of the adducts by Eq. (5) allowed us to calculate ΔH^0_{subl} for all the adducts and ΔS^0_{subl} for the silicon tetrafluoride and tetrachloride adducts. Comparison of the entropy characteristics of the adducts allowed estimation of ΔS^0_{subl} for $SiBr_4 \cdot 2Py$ (Table 5). Both the sublimation enthalpies and entropies are slightly higher than those for adducts of Group III element halides with pyridine [25]. This is likely to be explained by strong intermolecular interactions in the crystal state. Evidence for this assumption comes from the unusually high melting enthalpy of $SiCl_4 \cdot 2Py$ (128 kJ/mol [19]). The sublimation enthalpy increases along the series F, Cl, and Br, which agrees completely with the regularities characteristic of molecular compounds.

Table 5 lists the experimental temperatures at which the equilibrium constant of process (5) is equal to unit ($T_{K=1}$), and the calculated temperature at which the sublimation pressure is equal to 1 atm ($T_{p=1}$). Comparison of the $T_{K=1}$ values relating to complete dissociation of the complexes with the $T_{p=1}$ values relating to their sublimation shows that dissociation develops at temperatures 600–700 K lower than the

Table 5. Dissociation and sublimation characteristics of complexes $SiX_4 \cdot 2Py$

Complex	$\Delta H^0(3)$,[a] kJ/mol (calculation) (D_{2h})	$\Delta S^0(3)$, J mol^{-1} K^{-1} (calculation) (D_{2h})	$\Delta H^0(5)$,[a] kJ/mol (experiment)	$\Delta S^0(5)$, J mol^{-1} K^{-1} (experiment)	ΔH^0_{subl}, kJ/mol (D_{2h})	ΔS^0_{subl}, J mol^{-1} K^{-1} (D_{2h})	$T^{dis}_{K=1}$, K	$T^{subl}_{p=1}$, K
$SiF_4 \cdot 2Py$	89.1	329.2	273	490	183.9	160.8	557	1144
$SiCl_4 \cdot 2Py$	11.7	348.9	231	520	219.3	171.1	444	1282
$SiBr_4 \cdot 2Py$[b]	–6.9	348.3	237	(536)	243.9	(188)	(442)	(1297)

[a] $\Delta H^0(3)$ and $\Delta H^0(5)$ are the enthalpies of processes (3) and (5), respectively. [b] Values in parentheses are estimated.

sublimation temperature. Consequently, the adducts should not pass into vapor, which agrees well with experiment.

Calculation of the energy of donor–acceptor bond. The energy of a donor–acceptor bond is frequently estimated [26, 27] on the basis of the enthalpy of gas-phase dissociation on the assumption that the dissociation energy (or enthalpy) E_{dis} is equal to the total bond energy nE^b.

We showed in [3] that for a more correct description of bond energy one should take into account the distortion energies of the donor and the acceptor, which cannot be determined experimentally but can be calculated by modern quantum-chemical methods [28, 29]. With inclusion of these energies, the energy of a donor–acceptor bond can be found from Eq. (6).

$$nE^b_d(\text{Si–N}) = E_{dis} + [nE_{dis}(\text{Py}) + E_d(SiX_4)]. \quad (6)$$

Here n is the number of bonds, E^b_d(Si–N) is the Si–N bond energy calculated with inclusion of the distortion energy of the donor and the acceptor; E_{dis} is the gas-phase dissociation energy of the complex; E_d(Py) is the distortion energy of pyridine, and $E_d(SiX_4)$ is the distortion energy of silicon tetrahalide.

However, because of the limited basis set, in practice the calculated bond energy involves a basis set superposition error (BSSE) (for details, see [3, 28]). With inclusion of this error, the equation for bond energy takes form (7).

$$nE^b_d(\text{Si–N})^{BSSE} = E_{dis} + [nE_d(\text{Py}) + E_d(SiX_4)] + [nE(\text{Py})^{BSSE} + E(SiX_4)^{BSSE}]. \quad (7)$$

Here $E^b_d(\text{Si–N})^{BSSE}$ is the bond energy calculated with inclusion of the donor and acceptor distortion energies and BSSE.

As shown in [3], E^b_d(Si–N) in Eq. (6) represents an upper, and $E^b_d(\text{Si–N})^{BSSE}$ in Eq. (7), a lower limit of possible E^b(Si–N) values.

The E_d, E^{BSSE}, E_{dis}, and the energies of the chemical bond silicon–nitrogen E^b(Si–N), determined from Eqs. (6) and (7), are given in Table 6. The bond energies calculated as an arithmetic mean between E^b_d(Si–N) and $E^b_d(\text{Si–N})^{BSSE}$ are presented in the last column of Table 6.

As seen from Table 6, the distortion energy of the acceptor fragment is maximal for *trans* isomers. It is equal to 270–280 kJ/mol and practically coincides with the distortion energy for *trans*-ammoniates [3]. The distortion energies for the D_{2d} and D_{2h} configurations of the acceptor fragment are close to each other.

The donor fragment in pyridine complexes changes stronger than in ammonia complexes [3], but the distortion energy of the donor does not exceed 4 kJ/mol. The E^{BSSE} value for pyridine is more negative than for ammonia. Therefore, here, as well as in the case of ammonia compounds [3], this is the distortion energy of the acceptor, which determines the possibility of existence of pyridine complexes of silicon halides.

It is necessary to note that the inclusion of the electrostatic repulsion energy of pyridine molecules in the 1 : 2 complexes increases the Si–N bond energy by 4 (*trans* isomers of D_{2d} symmetry), 5 (*trans* isomers of D_{2h} symmetry), and 12–14 kJ/mol (*cis* isomers).

The energy of the donor–acceptor bond decreases in the series F, Cl, and Br for all types of complexes, changing within 105–225 kJ/mol. The strongest bonds take place in the 1 : 1 compounds, and the weakest, the *cis* isomers of the 1 : 2 compounds. However, the benefit from bond formation does not compensate for the expenses on acceptor distortion, and, as a result, the dissociation of monopyridine chloride and bromide adducts appears exothermic. Similarly, the low Si–N bond energies in combination with the high distortion energy result in that the dissociation of the *cis* forms of the chloride and bromide dipyridine adducts is energetically favorable. The *trans* forms are the only where the higher bond energy compensates

Table 6. Calculation of donor–acceptor bond energy (kJ/mol)

Adduct	E_d(Py)	E_d(SiX_4)	E(Py)^{BSSE}	E(SiX_4)^{BSSE}	E_{dis}	E_d^b(SiN)	E_d^b(SiN)^{BSSE}	E^b(SiN)^b
$SiF_4 \cdot Py_{ax}$	1.4	90.2	–5.9	–13.0	43.8	135.4	116.6	126 ± 11
$SiF_4 \cdot Py_{eq}$	3.3	220.3	–6.9	–13.4	11.7	235.3	215.0	225 ± 10
$SiCl_4 \cdot Py_{eq}$	4.1	220.3	–7.6	–10.5	–46.3	178.1	160.0	169 ± 9
$SiBr_4 \cdot Py_{eq}$	4.1	204.3	–7.9	–9.2	–51.1	157.3	140.2	149 ± 9
cis-$SiF_4 \cdot 2Py$	1.8	223.3	–7.2	–26.0	83.1	155.0	134.8	145 ± 10
cis-$SiCl_4 \cdot 2Py$	1.7	253.1	–8.1	–20.7	–4.2	126.2	107.7	117 ± 9
cis-$SiBr_4 \cdot 2Py$	1.8	248.2	–8.8	–17.4	–21.4	115.2	97.7	107 ± 9
trans-$SiF_4 \cdot 2Py$ (D_{2h})	2.7	272.1	–7.4	–25.5	103.1	190.3	170.2	180 ± 10
trans-$SiCl_4 \cdot 2Py$ (D_{2h})	2.2	282.1	–7.7	–22.7	27.0	156.8	137.7	147 ± 10
trans-$SiBr_4 \cdot 2Py$ (D_{2h})	2.2	269.1	–8.3	–17.7	8.4	141.0	123.8	132 ± 9
trans-$SiF_4 \cdot 2Py$ (D_{2d})	2.9	272.3	–7.2	–27.1	106.0	192.1	171.3	182 ± 11
trans-$SiCl_4 \cdot 2Py$ (D_{2d})	2.2	281.7	–7.7	–22.7	27.1	156.6	137.6	147 ± 10
trans-$SiBr_4 \cdot 2Py$ (D_{2d})	2.1	270.3	–8.3	–19.7	7.4	141.0	122.8	132 ± 9

[a] The bond energies are given without inclusion of the energy of electrostatic repulsion of two pyridine molecules. [b] The bond energy is the mean of E_d^b(SiN) and E_d^b(SiN)^{BSSE}.

for the expensed on fragment distortion. In this respect, the most favorable situation takes place with the silicon fluoride adducts in which the bond energy is much higher than in the other halide adducts.

Effect of ligand nature on structural and energy characteristics of $SiX_4 \cdot n$L adducts. The relative donor capacity of ammonia and pyridine, i.e. their relative strength as Lewis bases, changes depending on the reaction medium. In aqueous solutions, pyridine (pK 5.21) acts in relation to proton as a weaker base than ammonia (pK 9.2). On the contrary, the gas-phase basicity, i.e. proton affinity, of pyridine is mich higher (922.15 kJ/mol) compared with ammonia (857.73 kJ/mol) [30]. Gaseous pyridine behaves as a stronger donor also in relation to Group III element trihalides [31]. However, the Gutmann donor number *DN* of ammonia [32] is higher than that of pyridine by 1–2 units.

The effect of ligand L on the stability of adducts should be considered using stable structurally similar complexes as an example. Since 1 : 1 ammonia complexes are axial isomers and the corresponding pyridine complexes are equatorial isomers, their comparison makes no sense. For octahedral 1 : 2 complexes, *trans* isomers are the most stable both with ammonia and with pyridine, and, therefore, we will further dwell on these forms of complexes.

Characteristics of the *trans* forms of ammonia and pyridine $SiX_4 \cdot 2$L adducts are compared in Table 7 and Fig. 3. Since the characteristics of the D_{2h} and D_{2d} pyridine adducts are close to each other (Tables 2 and 4), we took for comparisons the D_{2h} adducts.

Analysis of data in Table 7 shows that replacement of ammonia by pyridine does not result in unidirectional changes in characteristics.

Comparison of the experimental dissociation enthalpies of crystalline adducts into components in the standard states $\Delta H^0_{f(stand.)}$ shows that the ammonia adduct $SiF_4 \cdot 2NH_3$ [$\Delta H^0_{f(stand.)}$ –229 kJ/mol] is more stable than the pyridine adduct [$\Delta H^0_{f(stand.)}$ –193 KJ/mol]. However, in the standard state ammonia is gaseous and pyridine is liquid. Therefore, with account for the vaporization enthalpy of pyridine, we pass to the characteristics of process (5) [ΔH^0(5)], which show that pyridine complexes are more stable. Finally, using the calculated enthalpies of homogeneous gas-phase reactions (3) [ΔH^0_{298}(3)] as the stability characteristics of the adducts, we have to accept that ammonia is a stronger donor in relation to silicon tetrahalides than pyridine (Table 7 and Fig. 3a). It results in shorter and stronger Si–N bonds in ammonia complexes compared to pyridine complexes (Table 7).

The distortion energy of acceptor SiX_4 is more sensitive to the nature of element X than to the nature of the donor: It changes only slightly in going from ammonia to pyridine at fixed halogen. At the same time, the Si–X distances therewith increase (to the smallest extent in the case of chlorine and to the greatest extent in the case of fluorine).

The H···X contacts are of importance both in ammonia and pyridine complexes. Therewith, the H···X distances in $SiX_4 \cdot 2NH_3$ are shorter than in $SiX_4 \cdot 2$Py, which appears to promote ammonolysis with HX liberation.

Table 7. Comparison of characteristics of the *trans* forms of $SiX_4 \cdot 2NH_3$ and $SiX_4 \cdot 2Py$ adducts

Parameter	$SiX_4 \cdot 2NH_3$			$SiX_4 \cdot 2Py$ (D_{2h})		
	X = F	X = Cl	X = Br	X = F	X = Cl	X = Br
$-\Delta H^0_{f(stand.)}$(exp.)	229	–	–	193	122	123
ΔH^0(5)(exp.)	229	–	–	273	231	237
ΔH^0_{298}(3)	98.2	50.6	39.6	89.1	11.7	–6.9
ΔH^0_{subl}	122–130	–	–	183.9	219.3	243.9
$E_d(SiX_4)$	272.4	280.2	266.8	272.1	282.1	269.1
E^b(Si–N)	187.2	168.7	157.9	180	147	132
l_{Si-N}(calc.)	1.966	1.979	1.990	1.980	2.042	2.063
l_{Si-N}(exp.)	1.895	–	–	1.93	1.976	–
l_{Si-X}(calc.)	1.662	2.217	2.406	1.689	2.219	2.414
l_{Si-X}(exp.)	1.662, 1.667	–	–	1.64	2.183	–
$l_{H\cdots X}$	2.428	2.669	2.770	2.511	2.694	2.781
$\Delta q(SiX_4)$	–0.55	–0.64	–0.656	–0.496	–0.585	–0.622
Δq_{Si}	–0.198	0.213	0.087	–0.182	0.213	0.087
Δq_N	–0.003	0.081	0.042	–0.021	–0.025	–0.016
Δq_X	–0.088	–0.212	–0.181	–0.078	–0.199	–0.177
Δq_C	–	–	–	0.084	0.100	0.113
				–0.034	–0.034	–0.044
				0.025	0.028	0.033
Δq_H	0.068	0.073	0.067	0.059	0.061	0.058
	0.070	0.077	0.077	0.008	0.012	0.014
	0.070	0.077	0.77	0.008	0.011	0.012

The negative charge on SiX_4 increases in all the complexes (Fig. 3b), but the negative charge on silicon appears only in fluorides. The charge on the nitrogen atoms changes only slightly (Fig. 3c), and in pyridine adducts it is more negative than in ammonia adducts, i.e., in fact the nitrogen atom is thus rendered electron-acceptor instead of electron-donor. This is connected with essential charge redistribution on pyridine hydrogen and carbon atoms. The carbon atoms nearest to the nitrogen atom and to the formed donor–acceptor bond become much more positive. For example, in *trans*-$SiF_4 \cdot 2Py$, Δq_C increases by 0.8 (Table 7).

Ammonia and pyridine complexes are close to each other in the changes of the charge on Si and X atoms. The more negative charge is accumulated on X, the more positive becomes Si (Figs. 3d and 3e). In the series F, Cl, and Br, these dependences peak on the chlorine atom.

Thus, our calculations show that the donor–acceptor interaction involves all atoms in the donor and acceptor molecules.

Pyridine and ammonia [2] adducts of silicon tetrahalides have close distortion and bond energies. The energy of SiX_4 distortion for the axial isomers of the five-coordinate silicon complexes $SiX_4 \cdot L$ is 80–90 kJ/mol, whereas the respective value for *cis*- and *trans*-$SiX_4 \cdot 2L$ reach 200–280 kJ/mol. These values are higher by almost an order of magnitude than those for Group III element halides whose maximum distortion energy is 35 kJ/mol [29]. Such distinctions are connected with a more profound structural rearrangement of SiX_4 on complex formation.

In terms of the hybridization model, this points to a substantial energy consumption for involvement of vacant *d* orbitals into the formation of the sp^3d and sp^3d^2 hybrid orbitals of five- and six-coordinate silicon.

In terms of the model of hypervalent bonds [33–36], which is more frequently applied to these compounds, five- and six-coordinate silicon compounds contain one or two three-center four-electron bonds (Fig. 4).

The resulting distortion energies indicate that to pass from a tetrahedron with usual covalent bonds to a trigonal bipyramid or a pseudo-octahedron with

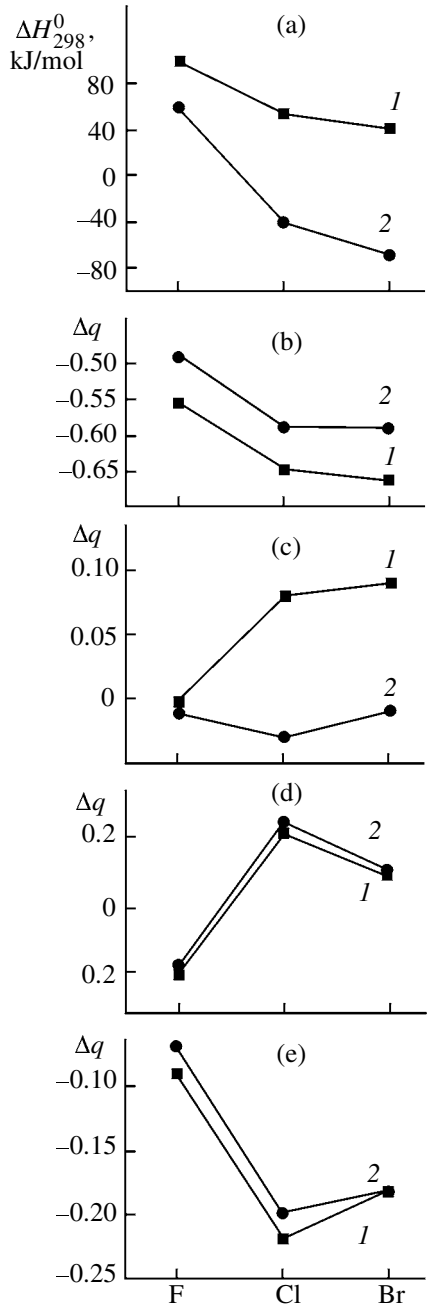

Fig. 3. (a) Dissociation enthalpies ΔH^0_{298} and (b–e) changes in effective atomic charges Δq for the *trans* isomers of complexes (*1*) $SiX_4 \cdot 2NH_3$ and (*2*) $SiX_4 \cdot 2Py$ [(b) SiX_4, (c) N, (d) Si, and (e) X].

hypervalent bonds requires a substantial energy consumptions. The calculated bond energies are nicely consistent with the model of hypervalent bonds which rank below in strength to covalent bonds. In fact, the energy of the Si–N bond in the axial isomers of $SiX_4 \cdot NH_3$ is ~80–90 kJ/mol, and in the equatorial isomers of $SiX_4 \cdot Py$ it increases up to 150–225 kJ/mol.

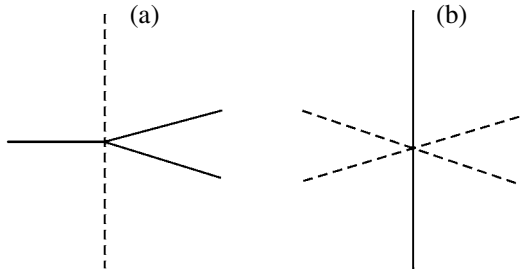

Fig. 4. Scheme of (solid line) covalent and (broken line) hypervalent bonds in (a) five-coordinate and (b) six-coordinate silicon complexes.

In the *trans* isomers of 1 : 2 adducts, the ligands are bound to the silicon central atom by strong covalent bonds whose energy span the range 158–187 kJ/mol for ammonia adducts and 130–180 kJ/mol for pyridine adducts. Thus, the energy of the Si–N bonds in the adducts under consideration fairly compares with the energy of the Al–N and Ga–N bonds in similar ammonia or pyridine complexes $MX_3 \cdot L$ (M = Al, Ga; L = NH_3, Py). These latter are stable adducts and could be observed experimentally in the gas phase {$\Delta H_{dis}(AlCl_3 \cdot NH_3)$ 137 [27] and $\Delta H_{dis}(GaCl_3 \cdot Py)$ 141 kJ/mol [31]}, whereas the dissociation enthalpy of $SiCl_4 \cdot Py_{eq}$ is –46.3 kJ/mol.

Our work showed that the reason for such a different behavior of tri- and tetrahalide adducts consists in a considerable (by about an order of magnitude) difference in the distortion energies: $E_d(AlCl_3)$ 28 and $E_d(SiCl_4)$ 220–280 kJ/mol. Thus, the high distortion energy of Group IV element halides determines the formation energy of their complexes and render them unstable despite the high energy of the donor–acceptor bond in the complexes.

ACKNOWLEDGMENTS

The work was financially supported by the Russian Foundation for Basic Research (project nos. 00-03-32566 and 01-03-06085).

REFERENCES

1. Sevast'yanova, T.N., Timoshkin, A.Yu., Davydova, E.I., Dubov, O.V., Suvorov, A.V., and Schaefer, H.F., *Zh. Obshch. Khim.,* 2003, vol. 73, no. 1, p. 52.
2. Timoshkin, A.Yu., Sevast'yanova, T.N., Davydova, E.I., Suvorov, A.V., and Schaefer, H.F., *Zh. Obshch. Khim.,* 2002, vol. 72, no. 10, p. 1674.

3. Timoshkin, A.Yu., Sevast'yanova, T.N., Davydova, E.I., Suvorov, A.V., and Schaefer, H.F., *Zh. Obshch. Khim.,* 2002, vol. 72, no. 12, p. 2019.
4. Rami, T. and Hensen, K., *J. Inorg. Nucl. Chem.,* 1971, vol. 33, no. 4, p. 937.
5. Feshin, V.P. and Kon'shin, M.Yu., *Zh. Obshch. Khim.,* 1995, vol. 65,, no. 5, p. 800.
6. Feshin, V.P. and Konshin, M.Yu., *Main Group Metal Chem.,* 1995, vol. 18, no. 2, p. 101.
7. Hensen, K., Stumpf, Th., Bolte, M., Nather, Ch., and Fleischer H., *J. Am. Chem. Soc.,* 1998, vol. 120, no. 40, p. 10402.
8. Frisch, M.J., Trucks, G.W., Schlegel, H. B., Gill, P.M.W., Johnson, B.G., Robb, M.A., Cheeseman, J.R., Keith,T., Petersson, G.A., Montgomery, J.A., Raghavachari, K., Al-Laham, M.A., Zakrzewski, V.G., Ortiz, J.V., Forestman, J.B., Cioslowski, J., Stefanov, B.B., Nanayakkara, A., Challacombe, M., Peng, C.Y., Ayala, P.Y., Chen, W., Wong, M.W., Andres, J.L., Replogle, E.S., Gomperts, R., Martin, R.L., Fox, D.J., Binkley, J.S., Defrees, D.J., Barker, J., Stewart, J.P., Head-Gordon, M., Gonzalez, C., and Pople, J.A., *GAUSSIAN 94*, Rev. C.3., Pittsburgh: Gaussian, 1995.
9. Becke, A.D., *J. Chem. Phys.,* 1993, vol. 98, no. 7, p. 5648.
10. Lee, C., Yang W., and Parr R.G., *Phys. Rev. B,* 1988, vol. 37, no. 2, p. 785.
11. *Modern Theoretical Chemistry,* Schaefer, H.F., Ed., New York: Plenum, 1976, vol. 3, p. 1.
12. Schafer, A., Horn H., and Ahlrichs, R., *J. Chem. Phys.,* 1992, vol. 97, no. 4, p. 2571.
13. Bain, V.A., Killean, R.C.G., and Webster, M., *Acta Crystallogr., Sect. B,* 1969, vol. 25, no. 1, p. 156.
14. Bechstein, O., Ziemer, B., Hass, D., Trojanov, S.I., Rybakov, V.B., and Maso, G.N., *Z. Anorg. Allg. Chem.,* 1990, vol. 582, no. 3, p. 211.
15. Ennan, A.A. and Kats, B.M., *Zh. Neorg. Khim.,* 1974, vol. 19, no. 1, p. 49.
16. Petrosyan, V.P., Ennan, A.A., and Kats, B.M., *Zh. Neorg. Khim.,* 1976, vol. 21, no. 9, p. 2363.
17. Aylett, B.J., Ellis, I.A., and Porritt, C.J., *J. Chem. Soc.,* 1972, no. 18, p. 1953.
18. Beatti, I.R. and Leigh C.J., *J. Inorg. Nucl. Chem.,* 1961, vol. 23, nos. 1–2, p. 55.
19. Konysheva, I.I., Sevast'yanova, T.N., and Suvorov, A.V., *Zh. Neorg. Khim.,* 1991, vol. 36, no. 5, p. 1260.
20. Vandrish, G. and Onyszchuk, M., *J. Chem. Soc. A,* 1970, no. 19, p. 3327.
21. Wannagat, U., Vielberg, F., and Voss, H., *Monatsh. Chem.,* 1969, vol. 100, no. 4, p. 1127.
22. Guertin, J.P. and Onyszchuk, M., *Can. J. Chem.,* 1969, vol. 48, no. 8, p. 1275.
23. Petrosyan, V.P., Ennan, A.A., and Konunova, Ts.B., *Zh. Neorg. Khim.,* 1978, vol. 23, no. 12, p. 3238.
24. Ennan, A.A. and Petrosyan, V.P., *Zh. Neorg. Khim.,* 1978, vol. 23, no. 12, p. 3381.
25. Sevast'yanova, T.N., and Suvorov, A.V., *Koord. Khim.,* 1999, vol. 25. no. 10, p. 727.
26. Gur'yanova, E.N., Gol'dshtein, I.P., and Romm, I.P., *Donorno-aktseptornaya svyaz'* (Donor–Acceptor Bond), Moscow: Khimiya, 1973.
27. Suvorov, A.V., *Doctoral (Chem.) Dissertaition,* Leningrad, 1977.
28. Timoshkin, A.Yu., Suvorov, A.V., and Schaefer, H.F., *Zh. Neorg. Khim.,* 2000, vol. 45, no. 3, p. 509.
29. Timoshkin, A.Y., Davydova, E.I., Sevastianova, T.N., Suvorov, A.V., and Schaefer, H.F., *Int. J. Quantum Chem.,* 2002, vol. 88, no. 4, p. 436.
30. Speranza, M., *Adv. Heterocycl. Chem.,* 1986, vol. 40, no. 1, p. 25.
31. Timoshkin, A.Yu., Suvorov, A.V., and Schaefer, H.F., *Zh. Obshch. Khim.,* 1999, vol. 69, no. 8, p. 1250.
32. Gutmann, V., *Coordination Chemistry in Non-aqueous Solutions,* Wien: Springer, 1968.
33. Kravchenko, E.A. and Buslaev, Yu.A., *Usp. Khim.,* 1999, vol. 68, no. 9, p. 787.
34. Tandura, S.N., Voronkov, M.G., and Alekseev, N.N., *Top. Curr. Chem.,* 1986, vol. 131, p. 99.
35. Shklover, V.B., Struchkov, Yu.T., and Voronkov, M.G., *Usp. Khim.,* 1989, vol. 58, no. 3, p. 353.
36. Gel'mbol'dt, V.O., *Koord. Khim.,* 1993, vol. 19, no. 9, p. 667.